Acta Crystallographica Section B
Structural Science
ISSN 0108-7681

Temperature-resolved study of the structural behaviour of nickel octahexyl phthalocyanine up to the liquid crystal transition

Madeleine Helliwell,[a]* Simon J. Teat,[b] Simon J. Coles[b,c] and William Reeve[d]

[a]Department of Chemistry, University of Manchester, Manchester M13 9PL, England, [b]Station 9.8, Daresbury Laboratory, Warrington, Cheshire WA4 4AD, England, [c]Department of Chemistry, University of Southampton, Highfield, Southampton SO17 1BJ, England, and [d]Diverse Technologies, Kingfisher House, Cambridge CB2 5EG, England

Correspondence e-mail:
mad@spec.ch.man.ac.uk

Received 11 April 2003
Accepted 1 July 2003

This paper describes a temperature-resolved crystallographic investigation into the behaviour of the title compound as the temperature is increased stepwise from room temperature up to 418 K, which is the temperature at which a transition to a discotic columnar mesophase takes place. The experiments were conducted using synchrotron radiation on Station 9.8 at the SRS at the Daresbury Laboratory. An intermediate transition to a less well ordered crystal form was seen at 326 K and differential scanning calorimetry (DSC) measurements confirmed the transition temperature of this change. Also, a new improved room-temperature crystal structure was obtained, as well as further structure determinations at 323, 328 and 353 K. These showed that as the mobility, particularly of the hexyl groups, increases with temperature, the packing of the molecules adjusts from pseudohexagonal layers to a rectangular arrangement.

1. Introduction

Phthalocyanines have many important commercial applications as pigments and catalysts. Their properties are dependent on their solid-state structures and in particular on their packing arrangements, and a compilation of known solid-state structures of phthalocyanines has appeared in recent reviews (Engel, 1997, 2003). We have focused on phthalocynines, which are highly substituted with long alkyl chains; such molecules with pentyl or longer alkyl chains can be thermotropic liquid crystals, with transitions to discotic columnar mesophases at elevated temperatures (Cook, 1994). We determined the first crystal structure of one such material, namely 1,4,8,11,15,18,22,25-octahexylphthalocyanine (Chambrier *et al.*, 1992). The molecules in the crystal are arranged in tilted stacks, which are widely spaced, with the shortest contact between the aromatic cores being 8.5 Å. Other packing arrangements are known to exist (Cook, 1994; McKeown, 1998), so we then investigated the crystal structure of (1,4,8,11,15,18,22,25-octahexylphthalocyaninato)nickel (1) to study the effect of metallation on the packing arrangement: this in fact turned out to be quite different to that of 1,4,8,11,15,18,22,25-octahexylphthalocyanine (Helliwell *et al.*, 1997). When crystal structures of (1) were determined at 295 and 103 K, the respective space groups were $C2/c$ and $P2_1/n$, with the phase transition occurring at *ca* 200 K. At room temperature the asymmetric unit contains two half molecules, with the Ni atom of one lying on a twofold axis, and of the other on a centre of symmetry; while at 103 K the asymmetric unit contains two complete molecules. However, the overall arrangement of the molecules at the two temperatures is similar and quite different to that of the unmetallated form; the molecules are arranged in approximately hexagonal arrays, with sheets of the crystallographically different molecules forming alternate layers and the lobes of the different molecules staggered with respect to one another. Perpendicular to the sheets of molecules, the aromatic cores form tilted stacks with the closest contact between the cores being 3.3 Å. This arrangement is in fact similar to the proposed structures of the mesophases formed at 418 and 437 K (Cherodian *et al.*, 1991); these were both tentatively assigned as D_{hd} from their textures. It was suggested that when the temperature increases, the hexyl groups become mobile, allowing free relative rotation of the molecules within the stacks (Helliwell *et al.*, 1997). Owing to the insight into the transition to the liquid crystal phase that crystal structures of (1) at 103 and 295 K have produced, further experiments were carried out to determine the changes to the structure which take place as the temperature is raised from room temperature up to the transition temperature. The results of these investigations are reported in this paper.

2. Experimental

A sample of (1) was donated by Professor M. J. Cook, from the University of East Anglia, and recrystallized by diffusion of hexane vapour into a dichloromethane solution.

2.1. Data collection

Data collection was carried out at Daresbury SRS, Station 9.8, using a wavelength of 0.6849 Å and a Bruker SMART 1k CCD diffractometer, by methods previously reported (Cernik *et al.*, 1997). Variation of the temperature at the sample was achieved using an Oxford Cryosystems Cryostream cooler for temperatures up to 373 K and a custom-built heating system for temperatures above 373 K. A series of 'snap-shots' was taken at temperatures from 293 to 418 K (*i.e.* up to the transition to the discotic columnar mesophase), see Fig. 1. These 'snap-shots' revealed that the diffraction patterns show little change up to a temperature of 323 K, but that there is a dramatic change in the patterns between 323 and 333 K, with higher mosaic spread, and a considerable reduction in resolution limit at the higher temperature. It was found that lowering the temperature back to 323 K did not reverse this alteration to the diffraction pattern, although subsequent differential scanning calorimetry (DSC) measurements suggested that this may be due to supercooling (see §2.3). Further studies on a different crystal using a stepwise rise of temperature in 1 K steps between 323 and 329 K showed that visible changes in the diffraction pattern started at 324 K and were greatest between 328 and 329 K. Above 329 K the diffraction pattern remained fairly stable until the crystal-to-mesophase transition at 418 K, but then the crystal started to visibly bend. At 418 K, the diffraction pattern no longer consisted of discrete spots and the transition to the liquid crystal phase had taken place. Four complete diffraction data sets were collected at 293, 323, 328 and 353 K. Exposure times of 1 or 2 s were used, and the data sets at 293 and 323 K were collected in approxi-

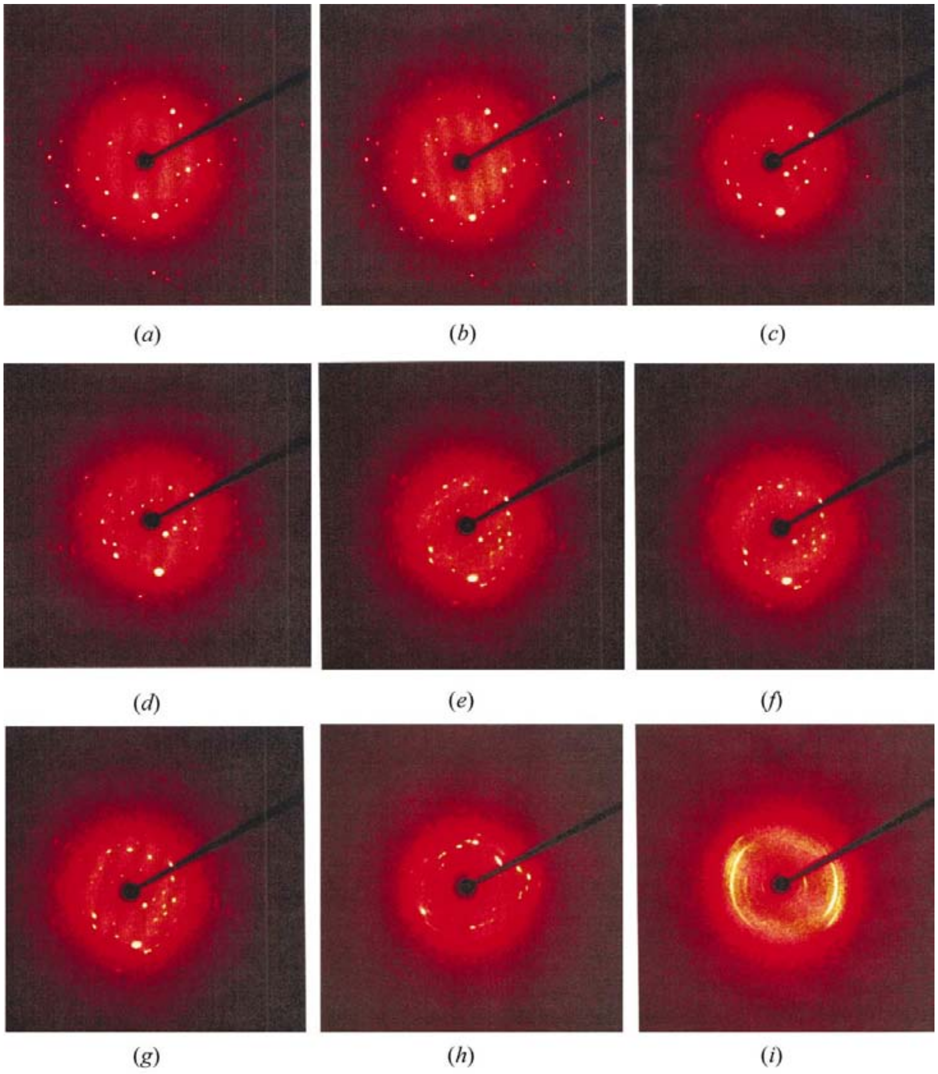

Figure 1
Snap-shots of the diffraction pattern at various temperatures: (*a*) 300, (*b*) 323, (*c*) 333, (*d*) 353, (*e*) 393, (*f*) 403, (*g*) 413 ($\varphi = 0°$), (*h*) 413 ($\varphi = 90°$) and (*i*) 423 K ($\varphi = 90°$).

Table 1
Crystal data.

Data for columns headed 293 K Station 9.8 and 295 K Cu *Kα* were obtained from Helliwell *et al.* (1997).

	103 K	293 K Station 9.8	295 K Cu *Kα*	323 K	328 K	353 K
Chemical formula	$C_{80}H_{112}N_8Ni$	$C_{80}H_{112}N_8Ni$	$C_{80}H_{112}N_8Ni$	$C_{80}H_{112}N_8Ni$	$C_{80}H_{112}N_8Ni$	$C_{80}H_{112}N_8Ni$
Formula weight	1244.52	1244.52	1244.52	1244.52	1244.52	1244.52
Space group	$P2_1/n$	$C2/c$	$C2/c$	$C2/c$	$C2/c$	$C2/c$
a (Å)	22.347	22.468 (3)	22.55 (2)	22.975 (16)	27.037 (7)	26.9247 (9)
b (Å)	37.246	37.010 (7)	37.14 (1)	36.38 (3)	33.449 (8)	33.391 (3)
c (Å)	18.834	18.942 (3)	18.994 (7)	18.926 (14)	19.117 (4)	19.1056 (12)
β (°)	115.185	114.518 (10)	114.60 (5)	115.266 (16)	121.65 (1)	121.471 (10)
V (Å^3)	14 186	14 331 (4)	14 463 (29)	14 307 (18)	14 764 (6)	14 650 (2)
Crystal size (mm)	0.5 × 0.03 × 0.01	0.9 × 0.04 × 0.015	0.55 × 0.07 × 0.03	0.9 × 0.04 × 0.015	0.9 × 0.06 × 0.01	0.9 × 0.06 × 0.01
Radiation type	Synchrotron	Synchrotron	Cu *Kα*	Synchrotron	Synchrotron	Synchrotron
Radiation wavelength (Å)	0.504	0.6874	1.5418	0.6874	0.6874	0.6874
θ max (°)	30.6	27.17	60.13	22.4	18.39	15.55
No. of reflections measured	85 873	44 215	12 794	26 273	15 272	10 633
No. of independent reflections	26 811	15 620	10 972	10 173	5888	3544
$R_{\rm int}$	0.055	0.103	0.136	0.105	0.128	0.249
No. of observed reflections	16 769	5808	3715	3409	2132	939
R	0.0687	0.0751	0.165†	0.0872	0.174	0.155
wR	0.212	0.210	0.135†	0.269	0.449	0.434
Tilt angle (°)	40.06	40.28		41.04	46.12	46.13

† This refinement was carried out on F; all others were based on F^2.

Table 2
Matrix of weighted r.m.s. deviations (Å) between data-set pairs measured at different temperatures.

Data set pairs (K)	103	295	323	328	353
103	–				
295	0.127	–			
323	0.247	0.130	–		
328	0.714	0.595	0.476	–	
353	0.760	0.640	0.520	0.196	–

mately 4 h, whilst those at 328 and 353 K took between 1 and 2 h because of the much higher mosaic spread. The resolution limits of the data sets decreased with temperature and those above 323 K were particularly difficult to process.

2.2. Refinements at different temperatures

Crystal data for the structures measured at 293, 323, 328 and 353 K are summarized in Table 1, together with those of the previously determined structures at 103 and 295 K (from Helliwell *et al.*, 1997). A *CHEMDRAW* image of (1) is shown in Fig. 2(*a*) and a plot of the 293 K crystal structure is shown in Fig. 2(*b*).

2.2.1. 293 K. The crystal structure refinement was initiated using the previously refined parameters of the structure measured at 295 K on an AFC-5*R* four-circle diffractometer equipped with a Cu *Kα* rotating anode source using *SHELXL*97 (Sheldrick, 1997). Anisotropic refinement was carried out on all non-H atoms except C62, with the H atoms included in calculated positions using the riding method. The atoms C21 and C22 were each disordered over two sites whose occupancies were constrained to sum to 1.0, with final occupancies of 0.36 and 0.64 for the *A* and *B* components, respectively. Some restraints were applied to the bond lengths in the hexyl chains. The new structure showed considerable improvement over the previous 295 K crystal structure measured on the AFC-5*R* diffractometer. In particular, there were 5808 reflections with $I > 2\sigma(I)$ and 5057 reflections with $I > 2.5\sigma(I)$, compared with 3715 with $I > 2.5\sigma(I)$ used previously in the refinement; moreover, the final conventional R value was 0.0751 compared with 0.165 previously (using observed data) to a $\theta_{\rm max}$ of 27.17°.

2.2.2. 323 K. Data were measured on the same crystal as for the 293 K data set and extended to $\theta_{\rm max}$ = 22.4°. The atoms C3–C5 of the phthalocyanine core of molecule 1 showed disorder over two sites, with occupancies constrained to sum to 1.0, and refining to 0.52 and 0.48 for the *A* and *B* components, respectively; C22 was also resolved into two disordered components *A* and *B* with occupancies of 0.34 and 0.66, respectively. Most non-H atoms, except C3–C5, were refined anisotropically using restraints on those of the hexyl groups. Restraints were also used in the refinement of the bond lengths and angles of the hexyl groups. The final R value was 0.0872, using 3409 reflections with $I > 2\sigma(I)$.

2.2.3. 328 K. The data were collected on a new crystal and only extended to $\theta_{\rm max}$ = 18.39°; the new crystal was required since the previous crystal had been heated to 353 K, which led to a reduction in the diffraction quality. The parameters of the structure determined at 323 K were used as a starting point and it was necessary to employ damping initially, as well as restraints on the anisotropic displacement parameters of the non-H atoms, and on the geometry of the hexyl chains and disordered regions. The core atoms N2 and C1–C3 were each disordered over two sites, as were C17–C19, C29–C30, C32, C64, C69–C71 and C75—C76; the occupancies of *A* and *B* components were fixed at 0.5 for N2, C1–C3, C17–C19 and C29–C30; for C69–C71 and C75–C76 the occupancies of the *A* and *B* components were fixed at 0.6 and 0.4, and those of C64 were fixed at 0.4 and 0.6, respectively. Atoms C40 and C68 could not be located. The disordered atoms were refined isotropically and H atoms were included in calculated positions where possible. The damping was removed for the final rounds of refinement. The final R value was 0.1743, using 2132 observed $[I > 2\sigma(I)]$ reflections.

2.2.4. 353 K. The data were collected from the same crystal as for the 328 K data set; it extended to $\theta_{\max} = 15.55°$ and there were only 939 reflections with $I > 2\sigma(I)$. The parameters of the refined structure at 328 K were used as a starting point and the method of refinement was similar; the same atoms were disordered with occupancies fixed as for the 328 K structure; atoms C40 and C68 were however located. Damping was required throughout, owing to the low data-to-parameter ratio. The final R value was 0.1546 using the observed data.

2.3. DSC measurements

DSC measurements were conducted on crystals (2.932 mg) of (1), firstly by heating the sample from 173 to 473 K and then cooling back down to 173 K, using a rate of 5 K min^{-1}. The results are shown in Fig. 3. During the heating of the sample an endothermic change was seen at 326.0 K, which coincides with the transition to a less well ordered crystalline form between 323 and 328 K, observed by monitoring the diffraction pattern around these temperatures. At 421.5 K there is a further endothermic change, presumably because of the transition to the discotic columnar mesophase. There is a shoulder on this peak at 429.6 K. During the cooling down, exothermic changes were observed at 422.9, 400.0 and 307.4 K. The changes at 421.5 and 429.6 K in the heating process agree reasonably well with those measured previously (Cook *et al.*, 1991), which were assigned from the textures, to crystal-to-mesophase and mesophase-to-mesophase transitions, respectively. The crystal-to-crystal transition at 326 K appeared to be irreversible based on the measured diffraction patterns. However, the

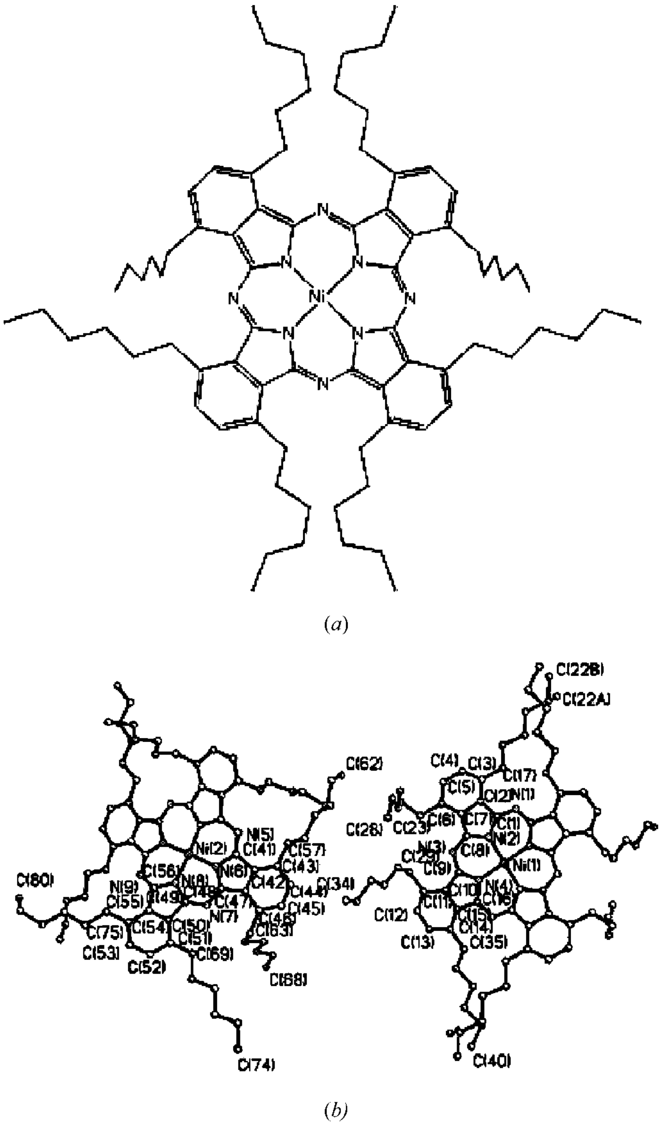

Figure 2
Plots of the crystal structure of (1) measured at 293 K. (*a*) *CHEMDRAW* image showing the connectivity and (*b*) showing the numbering scheme.

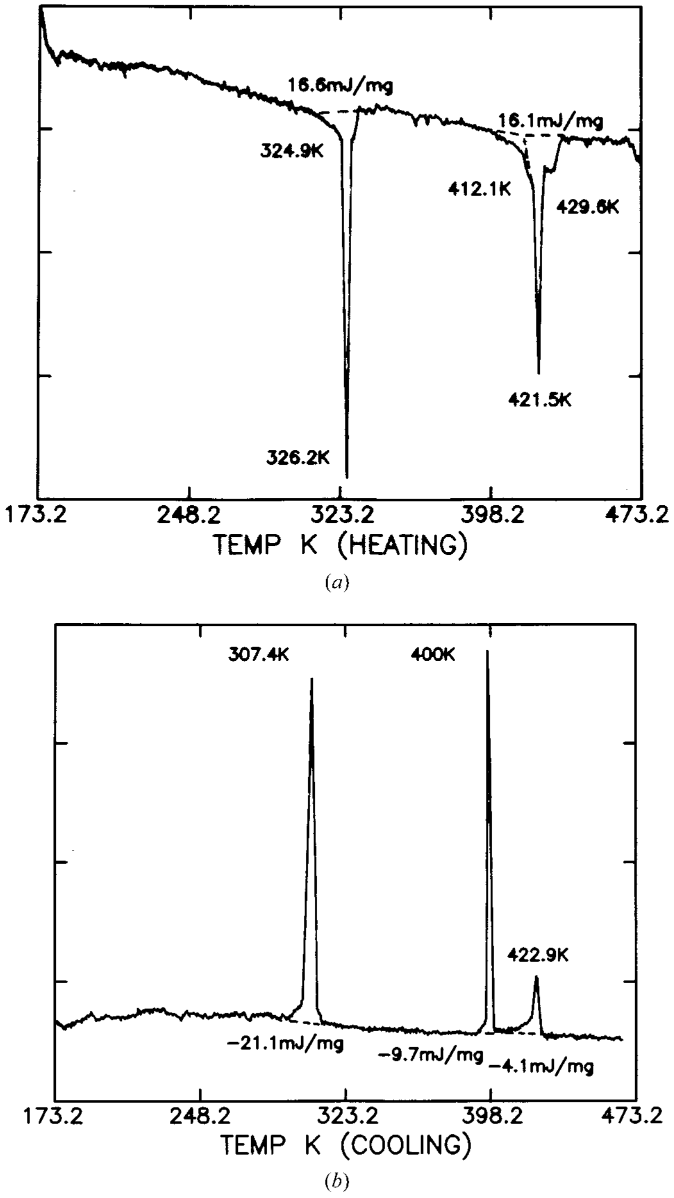

Figure 3
DSC using a temperature gradient of 5° min^{-1}: (*a*) heating and (*b*) cooling.

DSC results show that when the sample is cooled, there is an exothermic change at 307.4 K, suggesting that this transition may be subject to significant supercooling and explaining the apparent irreversibility of the change seen by monitoring the diffraction pattern; when the cooling rate was increased to 10 K min^{-1}, this transition occurred at 304.6 K. We intend to ascertain whether the crystal-to-crystal transition is reversible, but subject to a large hysteresis effect, in a future experiment and will publish the results separately.

2.4. Comparison of the temperature-resolved crystal structures

The crystal structures measured at the four different temperatures were compared by overlapping the equivalent Ni and N atoms in the crystal structures, using the OFIT command in *XP*, the graphics program from the *SHELXTL* package (Bruker, 2001). Weighted r.m.s deviations (Å) between the fitted atoms of data set pairs measured at different temperatures are shown in Table 2. Model-fitting plots are displayed in Fig. 4.

3. Results and discussion

Comparison of the refined crystal structures measured at 293 K with the original structure measured on the AFC-5*R* diffractometer at 295 K show that they agree very closely (Fig. 4*a*), with an r.m.s. difference, comparing Ni and N atoms of 0.0488 Å; there are some slight differences at the extremities of the hexyl groups, particularly where there is disorder and/or the thermal motion is high. Owing to the higher resolution and greater precision of the synchrotron radiation (SR) data set, the parameters derived from this refinement are clearly more reliable (the average C—C bond precision for the SR structure is 0.0093 *versus* 0.028 Å for the AFC-5*R* Cu *Kα* structure).

The similarity between the structure determined at 103 K and that measured at 293 K (Fig. 4*b*), and even to that at 323 K (Fig. 4*c*) is remarkable, especially since there is a change in space group from $P2_1/n$ to $C2/c$. One clear difference is that disorder appears in some of the core atoms of molecule 1 at 323 K. Raising the temperature further, however, does lead to a transition to a much less well ordered crystalline form, at 326 K, as measured by DSC; accompanying this transition is a marked change in unit-cell dimensions, a reduction of resolution and an increase in the mosaicity of the diffraction

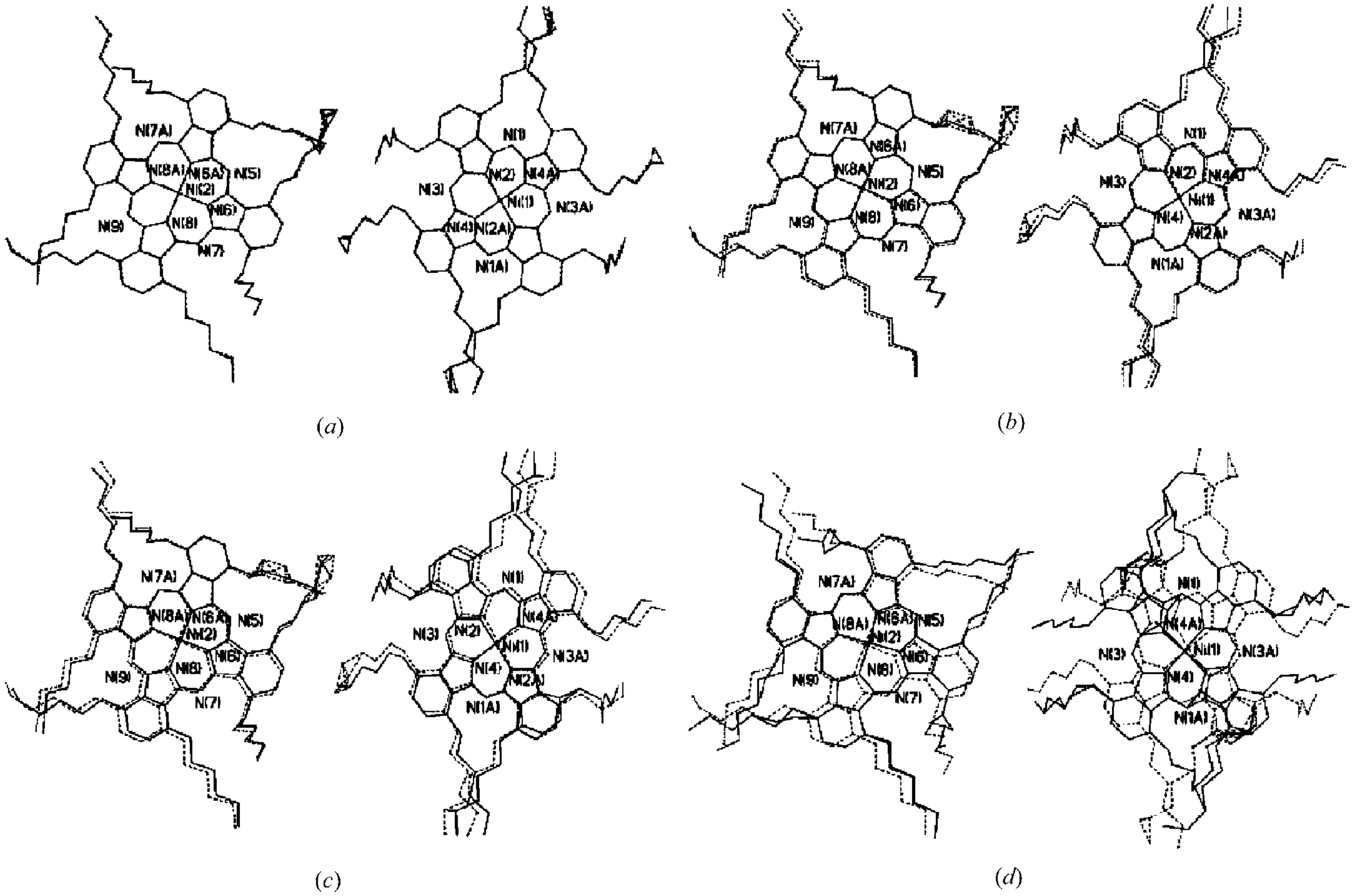

(*a*)

(*b*)

(*c*)

(*d*)

Figure 4

Overlap of Ni and N atoms of pairs of structures using OFIT. (*a*) Comparison of the Cu *Kα* 295 K crystal structure with the SR crystal structure measured at 293 K (dashed lines). (*b*) Comparison of the 293 K SR crystal structure (full lines) with the 103 K SR structure (dashed lines). (*c*) Comparison of the 323 K SR crystal structure (full lines) with the 103 K SR structure (dashed lines). (*d*) Comparison of the 328 K SR crystal structure (full lines) with the 323 K SR structure (dashed lines).

pattern, but the space group remains *C*2/*c*. Fig. 4(*d*) shows the overlap of the 323 and 328 K crystal structures. Refinement of the structures measured at 328 and 353 K could only be achieved using restraints on the geometric and displacement parameters, but the latter two structures are similar to each other (also indicated by their similar cell dimensions). Finally, no further transitions were observed in the DSC measurements, which supports our observation that there were no more obvious changes in the diffraction characteristics, until the transition to the first mesophase at 418 K.

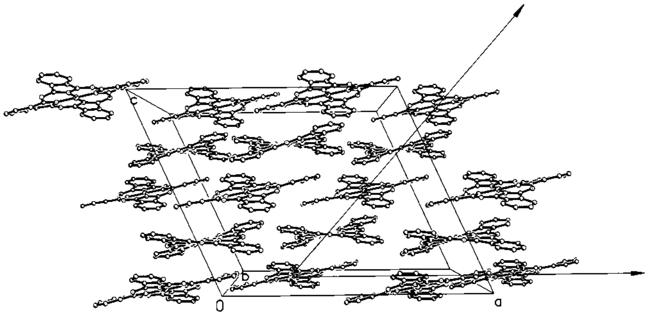

Figure 5
Plot displaying the tilted stacks for the 293 K SR crystal structure, with the hexyl groups omitted for clarity and with the tilt angle marked.

The jump in unit-cell dimensions which occurs at 326 K signifies a change in the packing of the molecules, in addition to the reduction in order of the structure and increased mobility, particularly of the hexyl groups; previously it was seen that molecules 1 and 2 are found in alternate layers, and that within each layer the molecules are arranged in a pseudohexagonal array (Helliwell *et al.*, 1997); for the new 293 K refinement, the Ni atoms are 21.6 and 22.5 Å apart (the latter being defined by the cell dimension *a*), with Ni—Ni—Ni angles of 58.7 and 62.5°. At 323 K the distances between Ni atoms are 21.5 and 23.0 Å, with angles of 57.7 and 64.5°. However, for the 328 K refinement the distances are 21.5 and 27.0 Å with angles 51.1 and 77.9° (with similar parameters for

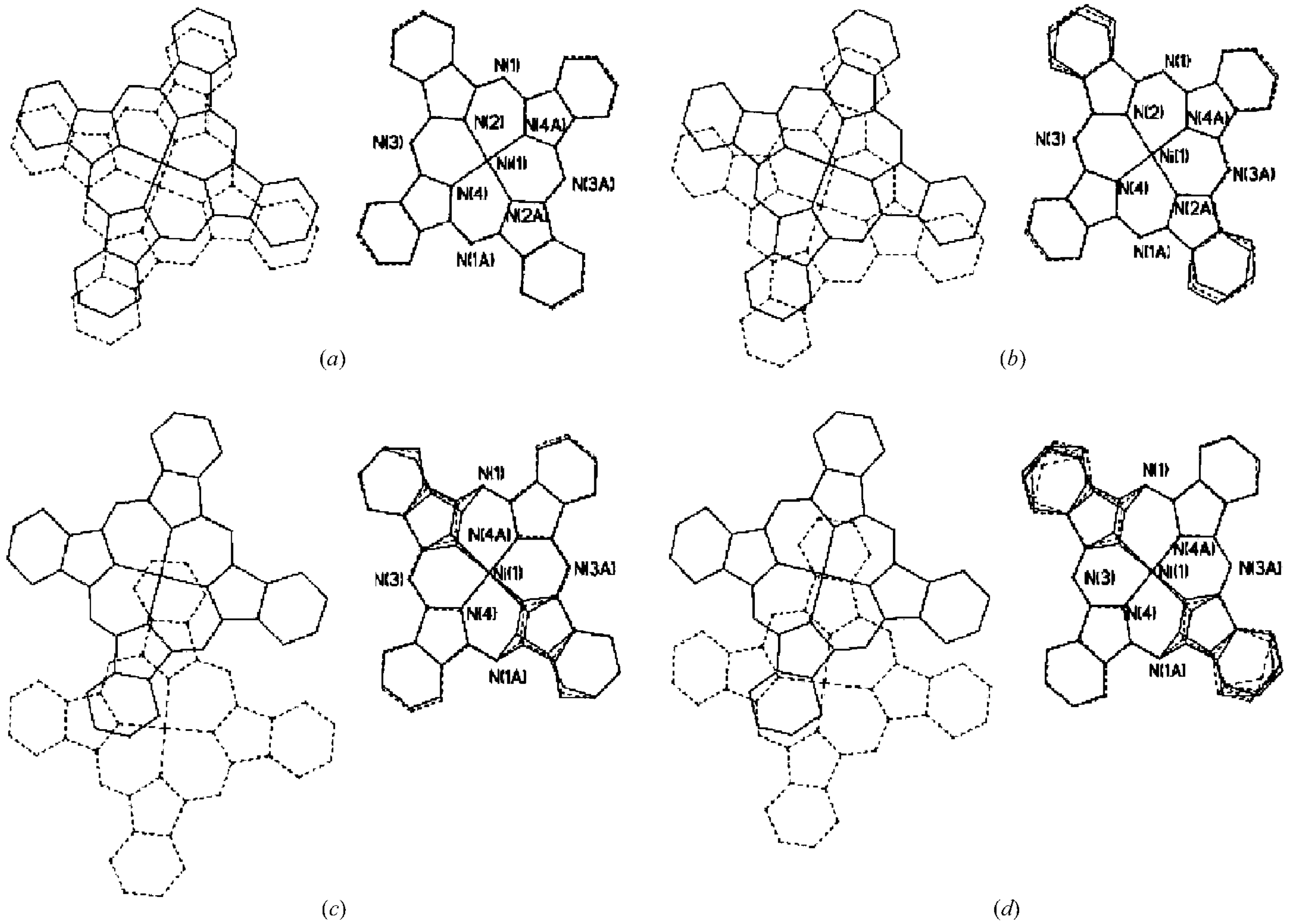

(*a*) (*b*)

(*c*) (*d*)

Figure 6
Relative displacement of molecule 2 between various temperature pairs, found by fitting Ni and N atoms of molecule 1 in OFIT (with hexyl groups omitted for clarity). (*a*) Overlapping molecule 1 of the 293 K SR crystal structure (full lines) with the 103 K SR structure (dashed lines). (*b*) Overlapping molecule 1 of the 323 K SR crystal structure (full lines) with the 103 K SR structure (dashed lines). (*c*) Overlapping molecule 1 of the 328 K SR crystal structure (full lines) with the 103 K SR structure (dashed lines). (*d*) Overlapping molecule 1 of the 328 K SR crystal structure (full lines) with the 323 K SR structure (dashed lines).

the 353 K structure). Thus, the layers of molecules are not pseudohexagonal for the 328 and 353 K structures and this is also indicated by the fact that the cell parameters no longer show the approximate relationship $a \simeq b \times 3^{1/2}$. The average spacing between layers of molecules is 1/4*c*, which slightly increases with temperature; at 103 K it is 4.71 Å and at 353 K it is 4.78 Å. However, the shortest contacts between atoms of adjacent layers are much shorter, owing to π-stacking interactions (3.3–3.4 Å). An angle of tilt can be defined by finding the Ni···Ni···Ni angle for three crystallographically equivalent molecules lying for example in the plane $y = 0.75$ and subtracting this from 90° to obtain the tilt angle from vertical (see Fig. 5). This increases with temperature, with the largest increase of 5.1° between the 323 and 338 K crystal structures (Table 1). By aligning the phthalocyanine ring of molecule 1 for different temperature pairs of structures, the relative displacement of Ni2 can be determined; Fig. 6(*a*) shows the 103 and 295 K pair, with a relative displacement of Ni2 of 0.94 Å; similarly, for the 103–323 (Fig. 6*b*), 103–328 (Fig. 6*c*) and 103–353 K pairs, the relative displacements are 1.67, 5.88 and 6.23 Å, respectively. The largest change in displacement arises between 323 and 328 K, where the relative displacement is 4.19 Å (Fig. 6*d*).

Previously, two mesophases were observed on cooling (1) from the isotropic liquid with transition temperatures of 437 and 418 K (Cherodian *et al.*, 1991); by viewing the textures of the two mesophases, they were both tentatively identified as D_{hd}; the D_{hd} assignment denotes discotic disordered hexagonal and the lower temperature phase had a more ordered needle texture, while that at higher temperature had a fan texture (Cherodian *et al.*, 1991). Our previous crystal structures at 295 and 103 K seemed to support this assignment, since the arrangement of the layers of molecules was pseudohexagonal (see above) and the cell dimensions showed the relationship that $b \simeq 3^{1/2} \times a$ (Helliwell *et al.*, 1997). However, the crystal structures measured at 328 and 353 K show that the layers of the molecules are no longer pseudohexagonal and cell dimensions are such that $b \simeq 1.24 \times a$, *i.e.* not hexagonal but rectangular. Fig. 7 shows a projection of a layer of molecule 2 in two dimensions, illustrating the rectangular arrangement. This in turn suggests that the mesophases might also be rectangular, with D_{rd} assignment rather than the D_{hd} assignment indicated by observing the textures of the mesophases. In order to investigate this proposal, powder diffraction experiments are planned, which will be reported separately.

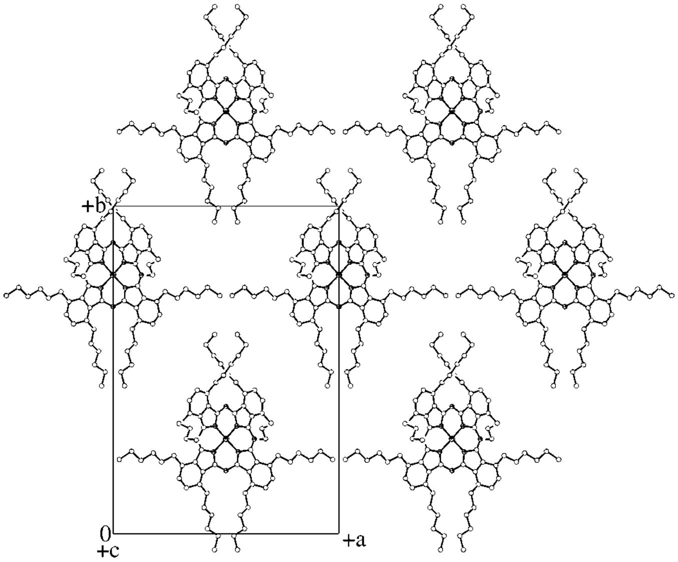

Figure 7
Projection of a layer of molecule 2 in two dimensions, showing the centred rectangular arrangement.

4. Concluding remarks

In summary, the changes in packing that take place with temperature are

(i) a change from pseudohexagonal cross-sectional symmetry to a rectangular arrangement;

(ii) an increase in the tilt angle as defined above;

(iii) an alteration in the relative positions of molecules 1 and 2.

In all cases, the adjustments are gradual up to the transition temperature of 326 K, with much larger modifications at this point which are nonetheless in the same direction.

These studies illustrate the power of modern SR crystallography, both in the accuracy and the speed of structures acquisition. Thus, a structural basis of the pathway to the liquid crystal transition itself is charted in detail; the transition from the crystal phase to the discotic columnar mesophase occurs in a number of transitions marking the stepwise reduction of order of the sample; as the hexyl groups start to 'melt', it is proposed that the molecules adjust towards the liquid crystal packing arrangement when the hexyl groups become completely mobile. This ensemble of experiments can now inform theoretical/computational 'molecular dynamic' studies of the impact of different functionalities and connects with other existing knowledge; this includes the substituent types and positions on the phthalocyanine rings as well as the possible inclusion of a central metal atom, and its type.

We thank Professor J. R. Helliwell, Dr N. B. McKeown and Professor M. J. Cook for discussions, and Professor M. J. Cook for donating the sample of (1). We are also grateful for the support of Daresbury SRS for the provision of synchrotron radiation facilities and M. Jennings for the DSC measurements.

References

Bruker (2001). *SHELXTL*. Version 6.12. Bruker AXS, Madison, Wisconsin, USA.

Cernik, R. J., Clegg, W., Catlow, C. R. A., Bushnell-Wye, G., Flaherty, J. V., Greaves, G. N., Burrows, I., Taylor, D. J., Teat, S. J. & Hamichi, M. (1997). *J. Synchrotron Rad.* **4**, 279–286.

Chambrier, I., Cook, M. J., Helliwell, M. & Powell, A. K. (1992). *J. Chem. Soc. Chem. Commun.* pp. 444–445.

Cherodian, A. S., Davies, A. N., Richardson, R. M., Cook, M. J., McKeown, N. B., Thomson, A. J., Feijoo, J., Ungar, G. & Harrison, K. J. (1991). *Mol. Cryst. Liq. Cryst.* **196**, 103–114.

Cook, M. J. (1994). *J. Mater. Sci. Mater. Electron.* **5**, 117–128.

Cook, M. J., Cracknell, S. J. & Harrison, K. J. (1991). *J. Mater. Chem.* **1**, 703–704.

Engel, M. K. (1997). *Report Kawamura Inst. Chem. Res.* pp. 11–54.

Engel, M. K. (2003). *The Porphyrin Handbook II*, edited by K. M. Kadish, K. M. Smith & R. Guilard, ch. 122, p. 20. New York: Academic Press, Elsevier Science Ltd.

Helliwell, M., Deacon, A., Moon, K. J., Powell, A. K. & Cook, M. J. (1997). *Acta Cryst.* B**53**, 231–240.

McKeown, N. B. (1998). *Phthalocyanine Materials Synthesis, Structure and Function*. Cambridge University Press.

Sheldrick, G. M. (1997). *SHELXL*97. University of Göttingen, Germany.